Supplement of

Sensitivities of mean and extreme streamflow to climate variability across Europe

Anna Luisa Hemshorn de Sánchez et al.

Correspondence to: Anna Luisa Hemshorn de Sánchez (a.l.hemshorndesanchez@vu.nl)

S1. Catchment area

Figure S1 shows the histogram of the catchment areas of the catchments used in the analysis.

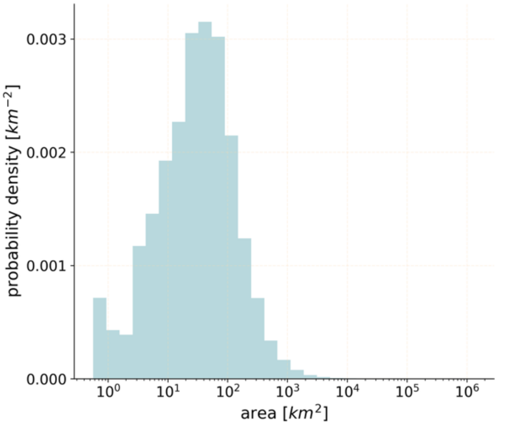

Figure S1: Histogram of the catchment area of the selected catchments

S2. Comparison of the multiple linear regression and the hierarchical linear regression

To increase the robustness of the elasticities and sensitivities computed in this study, we tested an additional approach to obtain streamflow elasticities to precipitation and streamflow sensitivities to temperature as shown in Figure S2. In a first step (Figure S2a), we normalize streamflow and mean precipitation timeseries with their long-term mean (of overlapping years). We do this for annual mean, annual maximum and annual minimum streamflow. For the precipitation we use annual mean precipitation. This method of calculating elasticities is referred to as “arc-elasticity” (Lerner, 1933), where the streamflow elasticity to precipitation describes the percentage variation of streamflow related to a 1% variation in precipitation.

$$\varepsilon = \left(\frac{dQ}{dP}\right)_{\bar{P},\bar{Q}} \frac{\bar{P}}{\bar{Q}} = \frac{Q-\bar{Q}}{P-\bar{P}}\frac{\bar{P}}{\bar{Q}} \; . \qquad (1)$$

Then, we plot the normalized precipitation values against the normalized streamflow values and conduct a linear regression (Figure S2b). Here, we use Theil-Sen (scipy.stats.theilslopes package in Python), which is less sensitive to outliers. This slope, for which we calculate the uncertainty range (at a 90% confidence interval), describes the elasticity (ε). If the slope has values larger than 1, we consider the elasticity as amplified, meaning that a variation in precipitation leads to a positive variation in streamflow that is percentage-wise larger than the precipitation variation (Figure S2b). If the slope is between 0 and 1, the elasticity is dampened, showing a positive response that is percentage-wise smaller than the precipitation variation. We define slopes that are smaller than 0, as reversed. For this method, the statistical significance is calculated using the certainty range of 90%, testing for the null hypothesis that zero is within this certainty interval. In a third step, we conduct a linear regression between the absolute temperature and the residuals from the streamflow elasticities to precipitation (Figure S2c). The slope of this line describes the temperature sensitivity of the streamflow.

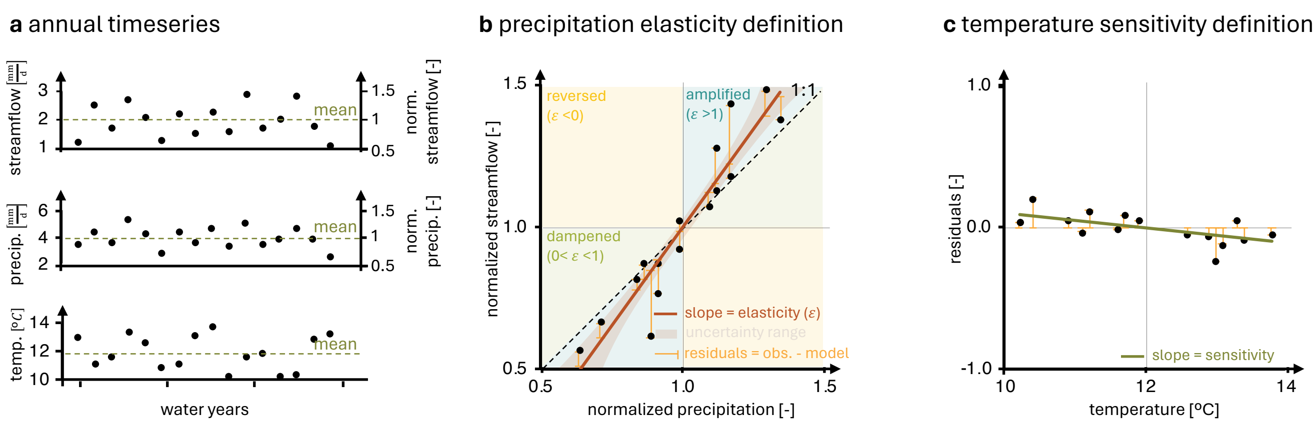

Figure S2: Methodology to estimate the streamflow elasticity to precipitation (slope) (a,b) and the streamflow sensitivity to temperature(a-c). The normalized timeseries streamflow and the normalized timeseries of precipitation (a) are used for the linear regression (b). The linear line that is fit through these points can be understood as the elasticity. The linear fit has its uncertainty range (transparent red). Depending on the value of the slope the elasticity is labelled as amplified, dampened or reversed (b). We use the absolute temperature (a), to explain the residuals of the elasticity to precipitation (b) to conduct a second linear regression (c). This slope expresses the temperature sensitivity of streamflow.

The results of the hierarchical linear regression are compared to the results of the multiple linear regression in Figure S3.

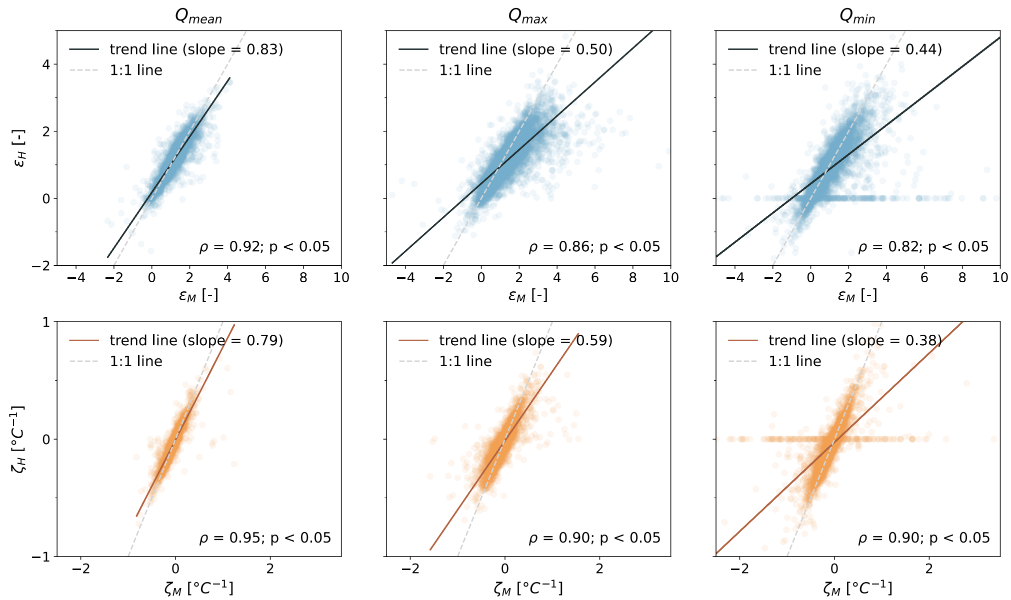

Figure S3: Comparison of annual elasticities to precipitation (upper row) and annual sensitivities to temperature (bottom row) for annual mean (left column), maximum (centre column) and minimum (right column) streamflow. The comparison shows that there is bias. This is mainly explained by the robustness towards outliers in the Theil-Sen regression of the hierarchical approach. This leads to lower values for the hierarchical approach because it is more robust towards extreme values. On the other side, for minimum flows this also means that if the timeseries contains many zero values the robust linear regression does not consider the few values that are not zero leading to an elasticity of zero, where the multiple linear regression still gives non-zero values.

S3. Comparison of streamflow elasticity to E-OBS station density

We use catchment-specific precipitation data from EStreams that is originally from E-OBS. The station density varies across Europe (Figure S4a). This can cause uncertainty to the precipitation data. To test whether the varying station density explains the spatial patterns we see in the streamflow elasticities (Figure S4b-d), we compute the correlation of the station density with the three annual streamflow elasticities (Figure S4e-f). The relationship is weak and somewhat more substantial for elasticities of annual maximum flow, but most of the geographic patterns in elasticity are unexplained by station density and seem to be driven by other factors.

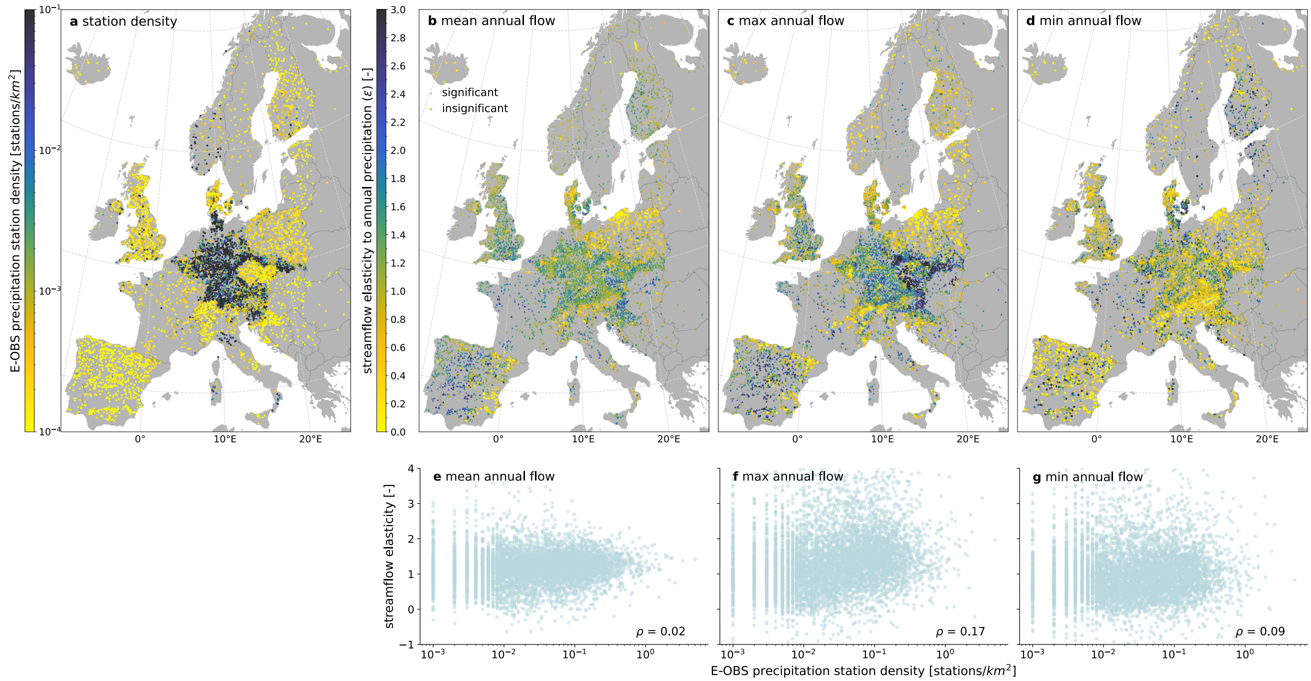

Figure S4: Maps of E-OBS precipitation station density (a), streamflow elasticity to annual precipitation of mean flow (b), max flow (c) and min flow (d) and comparison of the E-OBS precipitation station density to these three elasticities (e-g) with their corresponding spearman correlations. The map of the station density is set to a narrower colour range to show spatial differences more clearly, but maximum values range up to 1.7 as visible in plots e – g.

S4. Performance comparison of the multiple linear regression model

When analysing the model performance (R^2 in Figure S5) of the multiple linear regression model (using both precipitation and temperature) we see that it performs better than the sum of the individual models of only using precipitation or temperature. We also see that precipitation alone has a larger contribution to the model fit, while the temperature alone has a very low R^2. This is in line with (Masseroni et al., 2021) who found precipitation trends to be the main driver (over temperature) for streamflow trends in non-glacierized catchments in Europe. Similarly, (Woodhouse et al., 2016) found most of the variability of annual mean flows to be explained by cool season precipitation, but they also highlight that temperature can be highly influential under conditions like modest precipitation deficits. Further, the R^2 is much higher for the mean annual streamflow compared to the maximum and minimum annual flows.

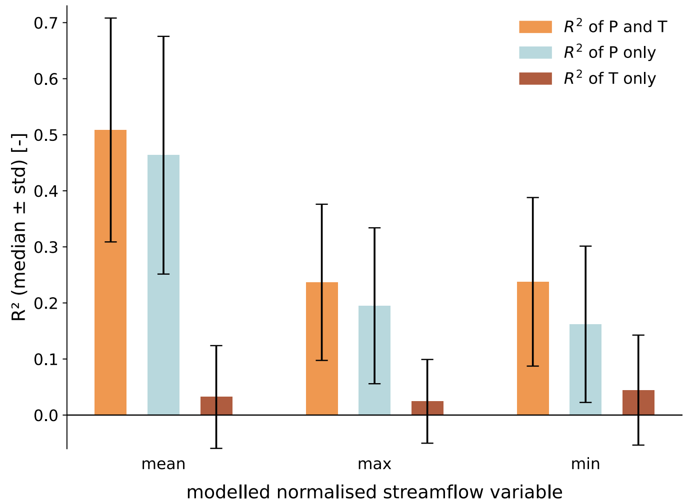

Figure S5: R^2 model performance using both precipitation and temperature (green), only precipitation (blue), and only temperature (orange) when modelling normalized mean (left), maximum (middle) and minimum (right) streamflow.

S5. Random Forest Model optimization

Based on the parameter optimization of GridSearchCV from scikit-learn we choose the parameters shown in Table S1 for the three models for the elasticities of annual mean, maximum and minimum flow to annual mean precipitation.

Table S1: Optimal hyperparameter values using the GridSearchCV from scikit-learn to model the target variables elasticities of mean, maximum and minimum annual streamflow.

Hyperparameter	**Target variable: Elasticity of**		
	Mean annual streamflow	Maximum annual streamflow	Minimum annual streamflow
Number of trees	500	500	500
Maximum depth	None	20	20
Minimum sample split	2	2	2
Minimum sample leaf	1	1	2

S6. Environmental Zones

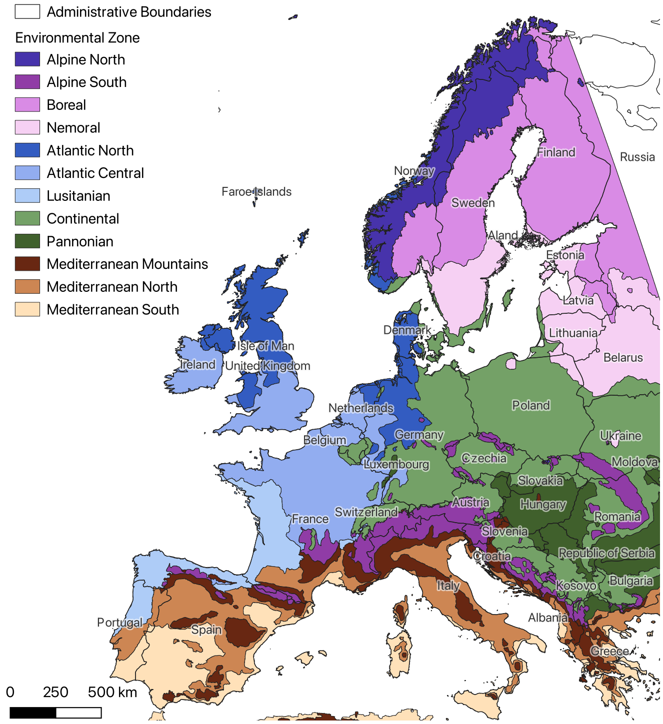

Figure S6: Environmental stratification (Metzger, 2018) and administrative boundaries of Europe

S7. Similarities of annual precipitation sensitivities of annual mean and maximum flows

In Fig. 2 we see that the elasticities of annual maximum flows to precipitation follow a similar spatial and frequency distribution to the ones of annual mean flows. In the regions of higher elasticities, the maximum flow is even more sensitive to mean annual precipitation that the mean annual flow. The two main hypotheses to explain this behaviour are

- (1): the mean precipitation of a hydrological year correlates with maximum precipitation or
- (2): wetter (drier) years lead to a wetter (drier) landscape that produces larger (smaller) maximum flows.

To test hypothesis (1), we compute the correlation of the mean precipitation to the maximum precipitation (Figure S7a). In the regions around the Sudeten and Carpathian Mountains, and the Eastern alps, with hotspots of high streamflow elasticities of maximum flow these correlations are higher. These are also regions where more streamflow occurs in the (early) summer period, as large amounts of precipitation fall on drier surfaces (Berghuijs et al., 2025). When comparing this correlation of annual mean and maximum precipitation with the elasticity of maximum flows to mean precipitation (Figure S7b), the relationship is very scattered. This indicates that across the scale of Europe, hypothesis (2) might play a more dominant role with some regions with summer dominated rainfall hypothesis (1) may contribute to higher elasticities.

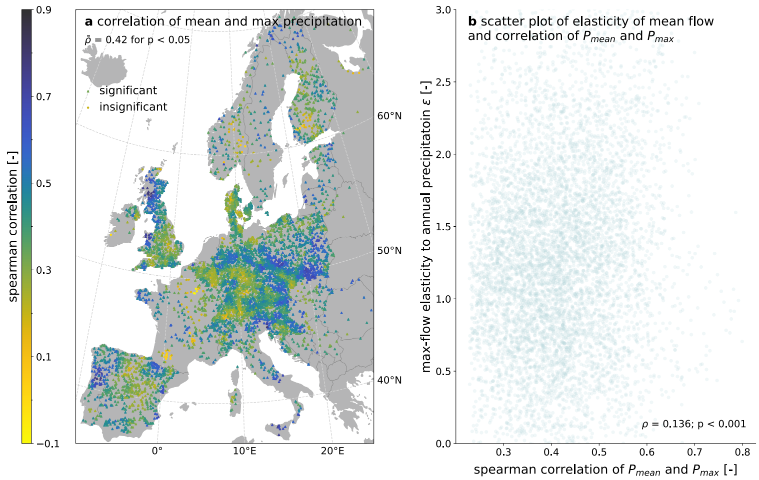

Figure S7: Geographical distribution of the correlation of maximum and mean precipitation (a) and comparison of this correlation to the elasticity of maximum flow to mean precipitation.

S8. Relation of seasonal dominance and annual centre of mass of streamflow

The emerging spatial patterns of seasonal dominance of elasticity of mean and maximum flow to precipitation resemble the pattern of streamflow seasonality (Berghuijs et al., 2025). As we are using the same seasons across Europe, it could be that the seasonal dominance is simply a representation of where the centre of mass of flow occurs throughout the year, meaning that if most of the precipitation occurs in the cold season it is cold-season dominated and if most of the precipitation falls in the warm season it is warm season dominated. To test this, we compare the centre of mass or mean day of the year of mean, maximum and minimum flows to the seasonal dominance (see Figure S8). If the seasonal dominance would only be based on the centre of mass, all catchments would fall in the upper field from October to May and in the bottom half from April to September. As this is not the case, there are likely additional factors influencing the seasonal dominance.

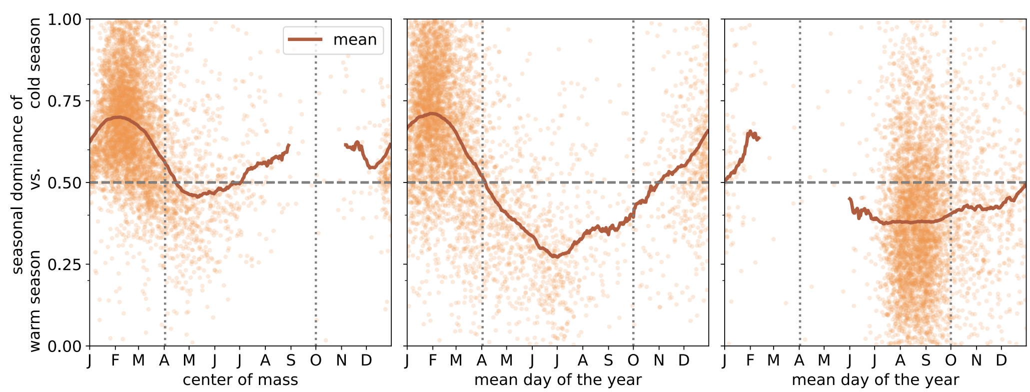

Figure S8: Comparison of seasonal dominance to centre of mass of mean annual flow (a), mean day of the year with maximum flow (b) or mean day of the year with minimum flow (c). The vertical dotted line indicates the boundaries of the cold and warm season. The redline shows the moving average.

S9. Spatial distribution of catchment characteristics

Here is an overview of the twelve most highly ranked catchment characteristics (Figure S9).

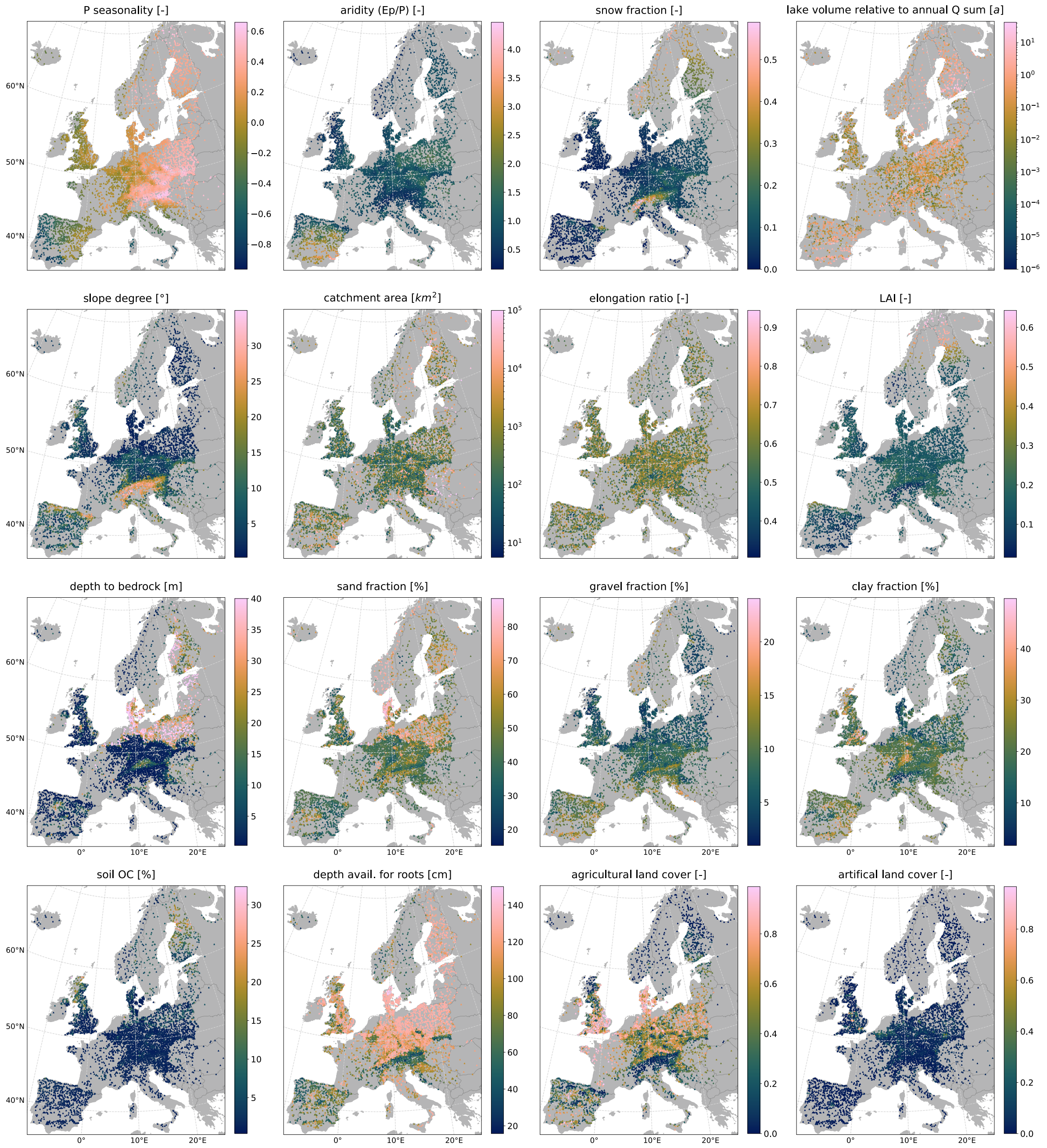

Figure S9: Spatial distribution of the most highly ranked features (characteristics) in the random forest model. Precipitation seasonality ranges from –1 (peak precipitation in the cold winter months), through 0 (precipitation evenly distributed throughout the year), to +1 (peak precipitation in the warm summer months). The relative lake volume and the catchment area are given in log scales.

S10. Importance of catchment characteristics considering the baseflow index

The baseflow index is a proxy for the contribution of groundwater to streamflow. It is more of a process description that influences elasticities rather than being a characteristic that influences a physical process. It could also be seen as an integrator of many different physical catchment characteristics (e.g. depth to bedrock, soil type, lake area, etc.).

When including the baseflow index to the analysis and thereby using 21 characteristics to model the annual streamflow elasticity to annual precipitation. The model predictions are only slightly higher compared to when not considering it ($R^2 \pm$ std: 0.57 ± 0.02), maximum (0.52 ± 0.02), and minimum flow (0.35 ± 0.03). This means that there are some processes described with the baseflow index that are not covered by the other 20 characteristics.

The baseflow index ranks distinctively highest for mean and minimum flow elasticities and is also among the higher-ranked characteristics for maximum flow elasticities. Maximum annual flows have likely a larger influence of fast runoff generation compared to mean and minimum flows, which could explain why the baseflow index is ranked lower for maximum flow elasticities. In catchments where the groundwater contribution to streamflow is larger and sufficiently slow, we could expect lower annual elasticities as the response time may be dominated by the slower responding groundwater (Karimi et al., 2023; Tegetmeyer et al., 2025). The negative relationship of the baseflow index to elasticities found here is in line with such behaviour.

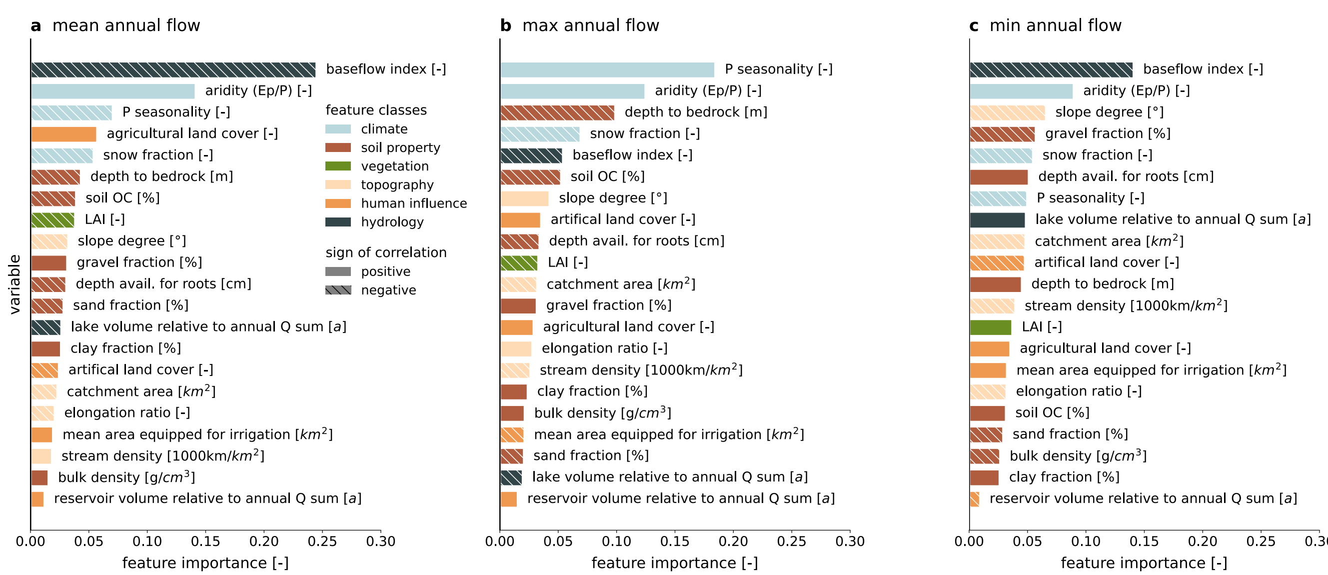

Figure S10: The role of catchment properties characteristics (including baseflow index) in shaping elasticities estimated by their feature importance for precipitation elasticities of mean (a), maximum (b) and minimum (c) annual streamflow to annual precipitation.

References

Berghuijs, W. R., Hale, K., and Beria, H.: Technical note: Streamflow seasonality using directional statistics, Hydrol Earth Syst Sci, 29, 2851–2862, https://doi.org/10.5194/hess-29-2851-2025, 2025.

Karimi, S., Leach, J., Karlsen, R. H., Seibert, J., Bishop, K., and Laudon, H.: Local- and network-scale influence of peatlands on boreal catchment response to rainfall events, Hydrol Process, 37, https://doi.org/10.1002/hyp.14998, 2023.

Lerner, A. P.: The Diagrammatical Representation of Elasticity of Demand, Rev Econ Stud, 1, 39–44, https://doi.org/10.2307/2967436, 1933.

Masseroni, D., Camici, S., Cislaghi, A., Vacchiano, G., Massari, C., and Brocca, L.: The 63-year changes in annual streamflow volumes across Europe with a focus on the Mediterranean basin, Hydrol Earth Syst Sci, 25, 5589–5601, https://doi.org/10.5194/hess-25-5589-2021, 2021.

Metzger, M. J.: The Environmental Stratification of Europe, https://doi.org/10.7488/ds/2356, 2018.

Tegetmeyer, C., Kaiser, M., and Barthelmes, A.: The European Wetland Map ('EWM’), https://doi.org/10.5281/zenodo.15302184, February 2025.

Woodhouse, C. A., Pederson, G. T., Morino, K., McAfee, S. A., and McCabe, G. J.: Increasing influence of air temperature on upper Colorado River streamflow, Geophys Res Lett, 43, 2174–2181, https://doi.org/10.1002/2015GL067613, 2016.